Available online at www.sciencedirect.com

ScienceDirect

Planetary and Space Science 56 (2008) 802–806

Planetary and Space Science

www.elsevier.com/locate/pss

Ionospheric photoelectrons at Venus: Initial observations by ASPERA-4 ELS

A.J. Coates[a,t,*], R.A. Frahm[b], D.R. Linder[a], D.O. Kataria[a], Y. Soobiah[a], G. Collinson[a], J.R. Sharber[b], J.D. Winningham[b], S.J. Jeffers[b], S. Barabash[c], J.-A. Sauvaud[d], R. Lundin[c], M. Holmström[c], Y. Futaana[c], M. Yamauchi[c], A. Grigoriev[c], H. Andersson[c], H. Gunell[e], A. Fedorov[d], J.-J. Thocaven[d], T.L. Zhang[f], W. Baumjohann[f], E. Kallio[g], H. Koskinen[h,g], J.U. Kozyra[i], M.W. Liemohn[i], Y. Ma[i,l], A. Galli[j], P. Wurz[j], P. Bochsler[j], D. Brain[k], E.C. Roelof[l], P. Brandt[l], N. Krupp[m], J. Woch[m], M. Fraenz[m], E. Dubinin[m], S. McKenna-Lawlor[n], S. Orsini[o], R. Cerulli-Irelli[o], A. Mura[o], A. Milillo[o], M. Maggi[o], C.C. Curtis[p], B.R. Sandel[p], K.C. Hsieh[p], K. Szego[q], A. Asamura[r], M. Grande[s]

[a] *Mullard Space Science Laboratory, University College London, Surrey RH5 6NT, UK*
[b] *Southwest Research Institute, San Antonio, TX 78228-0510, USA*
[c] *Swedish Institute of Space Physics, Box 812, S-98 128 Kiruna, Sweden*
[d] *Centre d'Etude Spatiale des Rayonnements, BP-4346, F-31028 Toulouse, France*
[e] *Department of Physics, West Virginia University, Morgantown, WV 26506-6315, USA*
[f] *Austrian Academy of Sciences, Space Research Institute, Graz, Austria*
[g] *Finnish Meteorological Institute, Box 503, FIN-00101 Helsinki, Finland*
[h] *Department of Physical Sciences, University of Helsinki, P.O. Box 64, FIN-00014 Helsinki, Finland*
[i] *Space Physics Research Laboratory, University of Michigan, Ann Arbor, MI 48109-2143, USA*
[j] *University of Bern, Physikalisches Institut, CH-3012 Bern, Switzerland*
[k] *Space Science Laboratory, University of California in Berkeley, Berkeley, CA 94720-7450, USA*
[l] *Applied Physics Laboratory, Johns Hopkins University, Laurel, MD 20723-6099, USA*
[m] *Max-Planck-Institut für Aeronomie, D-37191 Katlenburg-Lindau, Germany*
[n] *Space Technology Ireland, National University of Ireland, Maynooth, Co. Kildare, Ireland*
[o] *Instituto di Fisica dello Spazio Interplanetario, I-00133 Rome, Italy*
[p] *University of Arizona, Tucson, AZ 85721, USA*
[q] *KFKI Research Institute for Particle and Nuclear Physics, Budapest, Hungary*
[r] *Institute of Space and Astronautical Science, 3-1-1 Yoshinodai, Sagamichara, Japan*
[s] *Institute of Mathematical and Physical Sciences, University of Wales, Aberystwyth, Ceredigion, Wales, UK*
[t] *Centre for Planetary Sciences, University College London, London, UK*

Available online 31 December 2007

Abstract

We report the detection of electrons due to photo-ionization of atomic oxygen and carbon dioxide in the Venus atmosphere by solar helium 30.4 nm photons. The detection was by the Analyzer of Space Plasma and Energetic Atoms (ASPERA-4) Electron Spectrometer (ELS) on the Venus Express (VEx) European Space Agency (ESA) mission. Characteristic peaks in energy for such photoelectrons have been predicted by Venus atmosphere/ionosphere models. The ELS energy resolution ($\Delta E/E \sim 7\%$) means that these are the first detailed measurements of such electrons. Considerations of ion production and transport in the atmosphere of Venus suggest that the observed photoelectron peaks are due primarily to ionization of atomic oxygen.

Keywords: Venus; Plasma; Ionosphere

*Corresponding author.
E-mail address: ajc@mssl.ucl.ac.uk (A.J. Coates).
[l] Now at Institute for Geophysics and Planetary Physics, University of California, Los Angeles, California 90095-1567, USA

0032-0633/$ - see front matter © 2007 Elsevier Ltd. All rights reserved.
doi:10.1016/j.pss.2007.12.008

1. Introduction

The European Space Agency (ESA) Venus Express (VEx) spacecraft reached Venus on 11 April 2006. Shortly after arrival, characteristic peaks in the electron energy spectrum were observed by ASPERA-4 ELS in the Venus ionosphere. These were similar to those observed with Mars Express ASPERA-3 ELS at Mars (Frahm et al., 2006a). At Mars, the photoelectron energy peaks result from the ionization of atmospheric carbon dioxide and atomic oxygen by the helium 30.4 nm solar line, at an altitude in the atmosphere where vertical transport becomes significant. In this paper, we present and interpret VEx ELS data from 18 May 2006 which show evidence for ionospheric photoelectron peaks at Venus.

2. Background

The magnetic configuration at Venus is due to the solar wind interaction with this unmagnetized planet (Luhmann, 1995). A bow shock forms, where the solar wind slows, is heated and is deflected around the planet. The Interplanetary Magnetic Field (IMF) penetrates the shock and 'piles up' in front of the planet. The fields interact with the ionosphere as they are dragged around Venus (Luhmann and Cravens, 1991; Law and Cloutier, 1995).

Early measurements of the electron spectrum in the ionosphere of Venus were made on the Pioneer-Venus Orbiter (PVO). The Orbiter Retarding Potential Analyzer (ORPA) (Knudsen et al., 1979, 1980) measured the integral electron flux in the energy range 0–50 eV. Although these measurements gave the overall shape of the electron spectrum in the low-energy range, the ORPA data did not reproduce the sharp, characteristic peaks of atmospherically generated photoelectrons (Knudsen et al., 1980). Such peaks are seen in models of photoelectron production at Venus: the vertical transport model of McCormick et al. (1976), based on the Boltzmann equation, showed a single, broad peak in the 10–30 eV range. A two-stream model presented by Cravens et al. (1980) containing improved chemistry and higher energy resolution, showed that the single peak of McCormick et al. was actually a multiply peaked structure with three peaks in the 20–30 eV region of the spectrum. A further improvement, the two-stream model of Gan et al. (1990), predicted multiple (4) photoelectron peaks in the 20–35 eV region. Except for the fine structure in the measured electron spectrum, comparison between the measured and modelled spectra was favorable (Gan et al., 1990; Spenner et al., 1997).

When modelling Mars Viking data, Mantas and Hanson (1979) found peaks which appear at 21–24 eV and 27 eV, originating from the ionization of O and CO_2. The atomic and molecular ionization potentials of these are in close proximity: 13.62 eV (^{4}S), 17.10 eV (^{2}D), and 18.50 eV (^{2}P) for atomic oxygen and 13.77 eV ($X^2\Pi_g$), 17.32 eV ($A^2\Pi_u$), and 18.10 eV ($B^2\Sigma_u$) for carbon dioxide. Owing to the presence of O and CO_2 in the Venus atmosphere, the same ionization potentials apply. However, whereas at Mars the peaks were produced primarily through the ionization of CO_2, on Venus they were primarily produced by ionization of O, due to the lower altitude of the transition region between CO_2 and O at Venus (Schunk and Nagy, 2000). In addition, Mantas and Hanson modelled two cases of magnetic field orientation (horizontal and vertical) and found that there was an altitude (130–150 km on Mars) above which the atmosphere becomes transparent to the vertical transport of electrons. The most significant differences between Mars and Venus appear to be related to two considerations: (1) the altitude where vertical transport becomes important and (2) the dominant ion production rate at such altitudes.

3. Instrument

The VEx Electron Spectrometer (ELS) is an axially symmetric quadrispherical analyzer similar to that flown on Mars Express (Barabash et al., 2004). It has a field of view of $360^\circ \times 4^\circ$, with the 360° measurement plane divided into 16 sectors, each 22.5° wide. Laboratory calibrations to date give a value for the energy resolution ($\Delta E/E$) of 7% (as compared with the corresponding value of 8% for the MEx ELS) and a variation in the electrostatic analyzer conversion factor around the anode pattern varying between ~10.3 and ~11.4 eV/V (as compared with the corresponding MEx ELS value of 7.2 eV/V). The preliminary geometric factor of the VEx ELS is smaller than the MEx ELS value of 5.88×10^{-4} cm^2 sr (simulation and analysis are currently underway to estimate this). These differences are consistent with the smaller plate spacing and the small offset of the upper plate known to be characteristic of the VEx ELS (which is the MEx flight spare instrument). Additional information can be found in the Analyzer of Space Plasmas and Energetic Atoms (ASPERA-4) instrument paper by Barabash et al. (2007).

The ELS contains a dual range power supply with each range containing 4096 V (energy) steps. The voltage range varies from 0 V to approximately 21 V in its low range (about 200 eV maximum) and from 0 V to approximately 2800 V in its high range (about 30 keV maximum). For the observations shown in this paper, the VEx ELS covered the spectral range from 0.8 eV to 30 keV in 127 logarithmically spaced energy steps. The ELS protection grid was set at −5 V, thereby preventing electrons with energies less than 5 eV from striking the detector. Electron spectra were measured about every 4 s. As on MEx, the VEx ELS has variable energy ranges with different resolutions. Over/under energy sampling is available, but was not used for the observations shown here. The ASPERA-4 scanner, which increases the pitch angle coverage of ELS, is typically activated over a portion of most orbits. While this feature was not used in gathering the data reported in this paper, this capability will be exploited in future studies.

4. Data

The orbit of VEx on 18 May 2006 (2006 day 138) is shown in Fig. 1. It is plotted in Venus Solar Orbital (VSO) coordinates (Slavin et al., 1980). The orbital track is presented in a cylindrical system where the VSO Y and Z coordinates are used to form the radius. $\rho = (Y^2 + Z^2)^{1/2}$. The radius of Venus is $R_{\mathrm{Venus}} = 6052$ km. The average positions of the bow shock (blue) and ionopause (green) are marked and are determined from models by Biernat et al. (1999, 2000) and Luhmann (1992). Here the Sun is at the left and the VEx spacecraft enters the Venusian bow shock from the sunward side of the planet. During this pass, pericentre is on the nightside of Venus near the north pole terminator at 01:35:34 UT. The red bar indicates the time when ionospheric photoelectrons are observed (see below).

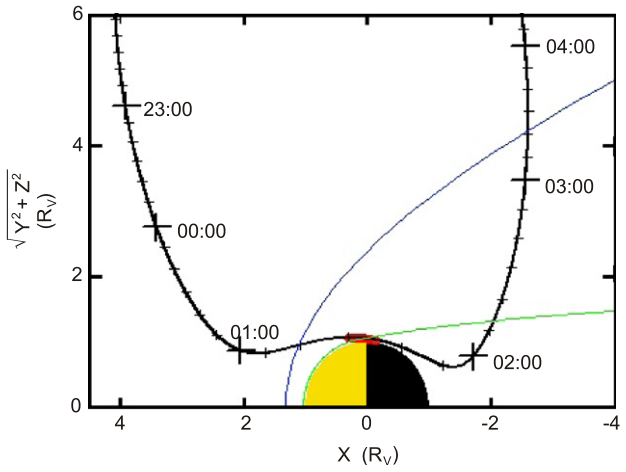

Fig. 1. Venus Express orbit on 18 May 2006 in Venus Solar Orbital (VSO) coordinates (Slavin et al., 1980), with the Sun to the left. The average bow shock (blue) and ionopause (green) positions are found from Biernat et al. (1999, 2000) and Luhmann (1992). Photoelectrons are observed during the time indicated by the red bar.

The electron data taken during the pass illustrated in Fig. 1 are shown in Fig. 2 as an energy-time spectrogram of count rate, which is proportional to differential energy flux. Only ELS sector 11 is used. The electron data begins in the solar wind. Possible foreshock electrons are seen at ~01:16 UT. At about 01:20 UT, the electron spectrum begins to change as upstream disturbances, probably related to the shock foot, are detected immediately upstream of the bow shock. At approximately 01:21:30 UT, the bow shock itself is encountered (the spacecraft altitude at that time was about 2500 km). The electron population is heated as it travels through the bow shock and shocked plasma from the sheath can thus be seen, which shows approximately the same intensity, until about 01:25 UT. At this point, the electron plasma begins to cool as the ambient intensity of intense energy flux decreases. At about 01:26:30 UT at an altitude of about 1300 km, the electron population begins to display a change in character from continuous sheath-like plasma to narrow beam-like structures. At about 01:28 UT at an altitude of about 900 km, these beam-like structures decrease in energy, and there appears to be a mixture of sheath and ionospheric plasma in a 'transition region'. Ionospheric plasma is continuously observed alone from about 01:30 UT and an altitude of 700 km. The transition region described is closely related to

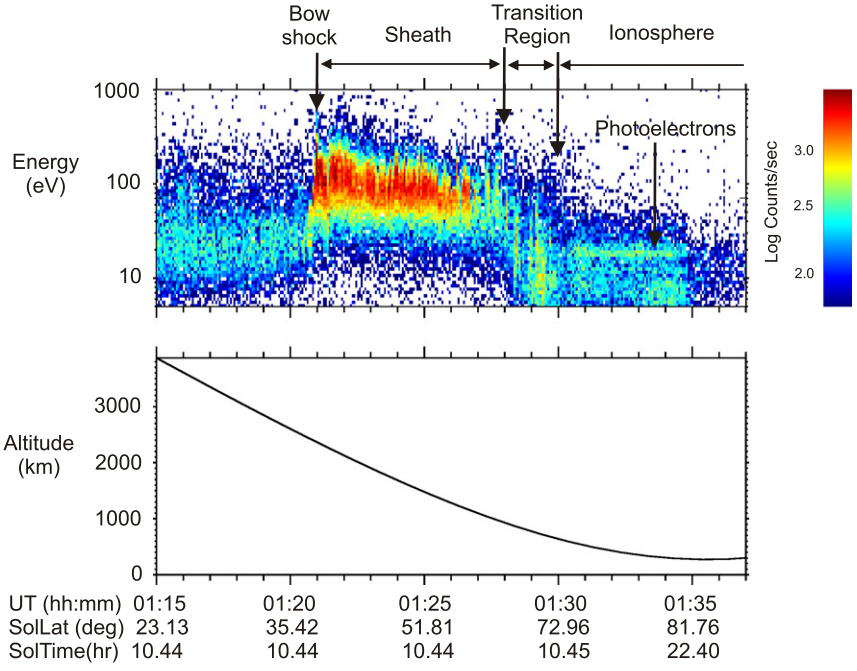

Fig. 2. Energy-time spectrogram of electron count rate (proportional to differential energy flux) for VEx ELS sector 11. Altitude is shown in the lower panel. The photoelectron peaks are seen as horizontal lines near about 18 eV between 01:30 and 01:35 UT.

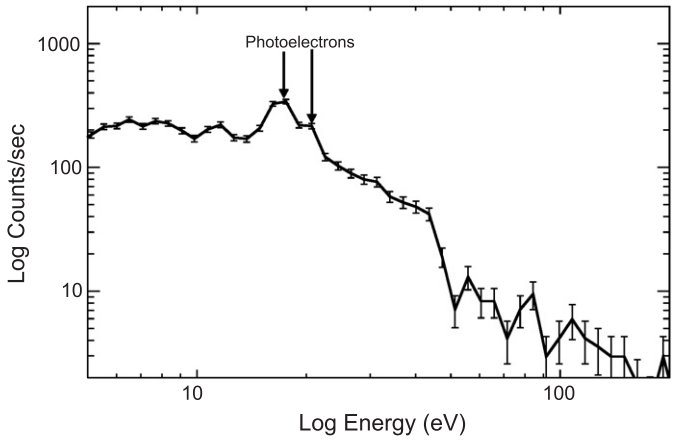

Fig. 3. Electron spectra (60) of counts, proportional to differential energy flux, are averaged between 01:30:30 and 01:34:32 UT. The photoelectron energy is nearly constant, indicating that spacecraft charging causes a constant energy offset in this period.

the 'plasma mantle' (Spenner et al., 1980) and 'magnetic barrier' (Zhang et al., 1991) regions and this topic will be studied elsewhere.

Ionospheric plasma showing peaks in the photoelectron spectrum is visible from 01:30 UT until approximately 01:35 UT; at which time the gradually increasing solar zenith angle (SZA) becomes greater than 97°. In the case of the Earth's ionosphere photoelectrons are detectable when the SZA is less than 97° (e.g., Coates et al., 1985). Slightly later than this at ~01:38 UT VEx enters into shadow, and nightside plasma is then detected until about 02:09 UT. The photoelectron peaks are observed as a horizontal line at about 18 eV between 01:30 and 01:35 UT. The steady energy level of the photoelectron peaks throughout this time indicates that the spacecraft potential is constant (approximately −5 V according to our analysis of photoelectron peaks, see also below).

The steady nature of the photoelectron spectrum for 5 min allows us to average to obtain better statistics. We averaged 60 4-s samples of the spectrum from sector 11 (from 01:30:30 UT) and the result is shown in Fig. 3. Using the simulated response function of the detector we have found that the observed intensity of the primary ionization peak (observed here at 22 eV) is highly dependent on the location and shape of the energy response of the detector relative to the narrow photoelectron peak. However, the observed spectrum in Fig. 3 shows a statistically significant peak/ledge feature at 22 eV (clearly visible also in Fig. 2), corresponding to the theoretical value of 27 eV (taking into account a −5 V spacecraft potential). The second observed peak is the more obvious and covers the 16–19 eV range. Correcting for spacecraft potential, we deduce that this peak is located between 21 and 24 eV. In addition to these characteristic spectral features, there is clear evidence for a rapid intensity decrease at high energies (~50 eV) as predicted by the model of Gan et al. (1990).

5. Discussion

In this example of photoelectron energy peaks at Venus, the signature of these peaks did not change in energy throughout the 5 min interval over which they were detected. This indicates that the influence on the spectrum due to charging of the spacecraft remained constant. During peak detection, the variation in spacecraft altitude was from about 700 km to about 250 km over the northern pole. The photoelectron peaks were observed inside the boundary of the ionosphere (ionopause). This boundary occurred at a higher altitude during this pass than was the case on average (Fig. 1).

Nagy and Cravens (1997) indicated that at Venus photoelectron transport can be neglected below 200 km. Above 165 km, the dominant ion is O^+. At 200 km, the production rate of O^+ ions is about 100 times greater than that of CO_2^+. Thus a significant number of photoelectrons liberated during ionization by He 30.4 nm photons can experience vertical transport. Densities of atmospheric and exospheric gases decrease approximately exponentially with altitude, thereby reducing the production rate of ambient ions, and therefore, the production rate of photoelectrons.

The process of local production is not as likely as that of transport because of the relatively low local neutral gas density available for photoionization and the nearly constant intensity of the measured photoelectron peaks. Thus for Venus, photoelectron peaks are inferred to be from O rather than from CO_2. This is opposite to the situation at Mars where the altitude at which transport becomes dominant is higher and the relative abundance of CO_2^+ relative to O^+ is greater (Mantas and Hanson, 1979). Therefore, the majority of electrons in the photoelectron energy peaks at Mars come from the photoionization of CO_2 (Frahm et al., 2006a).

If it is observed in other passes that atmospheric photoelectron peaks exist in the tail of Venus then, as at Mars, they can be used as tracers of the magnetic field (Frahm et al., 2006b; Liemohn et al., 2006). This can in turn indicate that the Martian crustal magnetic fields are unlikely to play a dominant role in the transport of photoelectrons away from the planet, since Venus has no crustal field, though at Mars they may modify where atmospheric photoelectrons are observed. Later studies of the pitch angle distribution of photoelectrons at the top of the ionosphere of Venus will reveal how such electrons are transported at Venus.

6. Summary

Photoelectron energy peaks due to ionization at 21–24 eV and at 27 eV were observed in the dayside ionosphere near the north pole of Venus. The ELS instrument which performed these measurements cannot directly discriminate between electrons generated by atomic oxygen and by carbon dioxide. However, based on

theoretical arguments, these signatures are likely to be electrons which are ionized from atomic oxygen in the Venusian upper atmosphere and subsequently transported to higher altitudes.

Acknowledgements

This work was supported in the UK by PPARC, in the USA by Southwest Research Institute and NASA Grant NNG04GH60G, and in Sweden by the Swedish National Space Board. We thank Neville Shane, Lin Gilbert and Gethyn Lewis of MSSL for analysis and plotting software. The ASPERA-4 team are grateful to NASA for allowing the ELS flight spare (constructed under contract NASW-00003) to be flown on Venus Express as part of ASPERA-4.

References

Barabash, S., et al., 2004. ASPERA-3: analyser of space plasmas and energetic ions for the Mars express. In: Wilson, A., Chicarro, A. (Eds.), Mars Express: The Scientific Payload. European Space Agency Special Report SP-1240, European Space Agency Research and Scientific Support. European Space Research and Technology Centre, Noordwijk, Netherlands, pp. 121–139.

Barabash, S., et al., 2007. The Analyzer of Space Plasmas and Energetic Atoms (ASPERA-4) for the Venus Express Mission. Planet. Space Sci. 55 (12), 1772–1792.

Biernat, H.K., et al., 1999. Aspects of MHD flow about Venus. J. Geophys. Res. 104, 12617–12626.

Biernat, H.K., et al., 2000. MHD effects in the Venus magetosheath. Adv. Space Res. 26, 1587–1591.

Coates, A.J., et al., 1985. Ionospheric photoelectrons observed in the magnetosphere at distances of up to 7 earth radii. Planet. Space Sci. 33, 1267–1275.

Cravens, T.E., et al., 1980. Model calculations of the dayside ionosphere of Venus: energetics. J. Geophys. Res. 85, 7778–7786.

Frahm, R.A., et al., 2006a. Carbon dioxide photoelectron energy peaks at Mars. Icarus 182, 371–382.

Frahm, R.A., et al., 2006b. Locations of atmospheric photoelectron energy peaks within the mars environment. Space Sci. Rev. 126 (1–4), 389–402.

Gan, L., et al., 1990. Electrons in the ionopause boundary layer of Venus. J. Geophys. Res. 95 (A11), 19,023–19,035.

Knudsen, W.C., et al., 1979. Retarding potential analyzer for the pioneer Venus orbiter mission. Space Sci. Instrum. 4, 351–372.

Knudsen, W.C., et al., 1980. Suprathermal electron energy distributions within the dayside Venus ionosphere. J. Geophys. Res. 85, 7754–7758.

Law, C.C., Cloutier, P.A., 1995. Observations of magnetic structure at the dayside ionopause of Venus. J. Geophys. Res. 100, 23973–23981.

Liemohn, M.W., et al., 2006. Mars global MHD predictions of magnetic connectivity between the dayside ionosphere and the magnetospheric flanks. Space Sci. Rev. 126 (1–4), 63–76.

Luhmann, J.G., 1992. Comparative studies of the solar wind interaction with weakly magnetized planets. Adv. Space Res. 12, 191–203.

Luhmann, J.G., 1995. Plasma interactions with unmagnetized bodies. In: Kivelson, M.G., Russell, C.T. (Eds.), Introduction to Space Physics. Cambridge University Press, Cambridge, pp. 203–226.

Luhmann, J.G., Cravens, T.E., 1991. Magnetic fields in the ionosphere of Venus. Space Sci. Rev. 55 (1–4), 201–274.

Mantas, G.P., Hanson, W.B., 1979. Photoelectron fluxes in the Martian ionosphere. J. Geophys. Res. 84, 369–385.

McCormick, P.T., et al., 1976. On the energy deposition of photoelectrons in the atmosphere of Venus. J. Geophys. Res. 81, 5196–5200.

Nagy, A.F., Cravens, T.E., 1997. Ionosphere: energetics. In: Bougher, S.W., Hunten, D.M., Phillips, R.J. (Eds.), Venus II. University of Arizona Press, Tuscon, pp. 189–223.

Schunk, R.W., Nagy, A.F., 2000. Ionospheres-Physics, Plasma Physics, and Chemistry. Cambridge University Press, Cambridge, pp. 433–443.

Slavin, J.A., et al., 1980. The solar wind interaction with Venus: pioneer Venus observations of bow shock location and structure. J. Geophys. Res. 85, 7625–7641.

Spenner, K., et al., 1980. Observation of the Venus mantle, the boundary region between the solar wind and ionosphere. J. Geophys. Res. 85, 7655–7662.

Spenner, K., et al., 1997. Photoelectron fluxes in the Venus dayside ionosphere. J. Geophys. Res. 102, 2577–2583.

Zhang, T.L., et al., 1991. The magnetic barrier at Venus. J. Geophys. Res. 96, 11,145–11,153.